

## Effects of substrate temperature and ambient oxygen pressure on growth of $\text{Ba}(\text{Fe}_{1/2}\text{Nb}_{1/2})\text{O}_3$ thin films by pulsed laser deposition

ZHANG Wei, WU ShuYa\* & CHEN XiangMing

Laboratory of Dielectric Materials, Department of Materials Science and Engineering, Zhejiang University, Hangzhou 310027, China

Received April 22, 2013; accepted June 5, 2013; published online July 11, 2013

$\text{Ba}(\text{Fe}_{1/2}\text{Nb}_{1/2})\text{O}_3$  thin films were grown on Pt/TiO<sub>2</sub>/SiO<sub>2</sub>/Si substrates with pulsed laser deposition (PLD) at temperatures ranging from 823 to 923 K with the varied ambient oxygen pressure. X-ray diffraction (XRD) data confirmed the single phase of polycrystalline  $\text{Ba}(\text{Fe}_{1/2}\text{Nb}_{1/2})\text{O}_3$  thin films. The effects of substrate temperature and ambient oxygen pressure on the surface morphologies of the thin films were investigated by atomic force microscopy (AFM) and the growth dynamics of thin films was discussed. Larger grains and denser surface morphologies were observed with increasing substrate temperature. While finer grains were produced with increasing ambient oxygen pressure due to more frequent collisions between the ejected species and ambient oxygen molecules. The influence of the substrate temperature and ambient oxygen pressure on the dielectric properties was also discussed. Improved dielectric constant and decreased dielectric loss was observed for the thin film deposited at evaluated temperature.

**$\text{Ba}(\text{Fe}_{1/2}\text{Nb}_{1/2})\text{O}_3$ , thin films, pulsed laser deposition, morphology**

**Citation:** Zhang W, Wu S Y, Chen X M. Effects of substrate temperature and ambient oxygen pressure on growth of  $\text{Ba}(\text{Fe}_{1/2}\text{Nb}_{1/2})\text{O}_3$  thin films by pulsed laser deposition. *Chin Sci Bull*, 2013, 58: 3398–3402, doi: 10.1007/s11434-013-5980-2

Complex perovskite  $\text{Ba}(\text{Fe}_{1/2}\text{Nb}_{1/2})\text{O}_3$  is a typical member in so-called giant dielectric constant materials, which are characterized by a very high dielectric constant step in the order of 103–105 over a broad temperature range with no detectable structure phase transition at the critical temperature where the abrupt change of dielectric constant is observed [1–6]. For their promising potential impact on shrinking and minimizing the microdevices, the giant dielectric constant materials have drawn much scientific attention over the recent years. Much effort has been made to understand the underlying physical origin of their unique dielectric behaviors. Both intrinsic and extrinsic mechanisms [7–11] have been brought up, though clear understanding is still a challenging issue. Our recent work on Raman spectra of  $\text{Ba}[(\text{Fe}_{1/2}\text{Nb}_{1/2})_{1-x}\text{Ti}_x]\text{O}_3$  solid solutions suggests local composition fluctuation in  $\text{Ba}(\text{Fe}_{1/2}\text{Nb}_{1/2})\text{O}_3$ , which may play an important role in the relaxor-like dielectric behaviors [12].

To better understand their dielectric behaviors and to realize their application, it is of considerable importance to synthesize giant dielectric constant thin films. One of the most widely employed techniques to prepare multicomponent thin films is pulsed laser deposition (PLD), which has its superior capacity to ensure the stoichiometric consistency of the target and the deposited thin films [13,14]. The previous investigations [15–18] have shown that the deposition conditions, such as substrate temperature, ambient oxygen pressure and laser settings have determinate impacts on the growth, crystal structure and physical properties of deposited thin films. To better control the physical properties and to get high quality thin films for investigation, it has great significance to study the impacts of key deposition conditions on the growth and the surface morphology of thin films.

In the present work,  $\text{Ba}(\text{Fe}_{1/2}\text{Nb}_{1/2})\text{O}_3$  thin films are prepared on Pt/TiO<sub>2</sub>/SiO<sub>2</sub>/Si substrates by PLD. The surface morphologies of thin films deposited in different conditions

\*Corresponding author (email: wushuya@zju.edu.cn)

are investigated by atomic force microscopy. The effects of substrate temperature and ambient oxygen pressure on the thin film growth are discussed and determined.

## 1 Experimental

Ba(Fe<sub>1/2</sub>Nb<sub>1/2</sub>)O<sub>3</sub> dense ceramic targets were prepared by a standard solid reaction route with high-purity BaCO<sub>3</sub> (99.93%), Fe<sub>2</sub>O<sub>3</sub> (99%) and Nb<sub>2</sub>O<sub>5</sub> (99.99%) powders as raw materials. The weighted materials were mixed and ball milled with zirconia media in diluted water for 24 h. The dried mixtures were calcined at 1473 K for 3 h in air. The calcined powders were ground and mixed with 6 wt%–8 wt% polyvinyl alcohol (PVA) water solution, and were dried and pressed into the cylindrical compacts. Finally, the dense Ba(Fe<sub>1/2</sub>Nb<sub>1/2</sub>)O<sub>3</sub> ceramics were obtained by sintering at 1773 K in air for 3 h.

Ba(Fe<sub>1/2</sub>Nb<sub>1/2</sub>)O<sub>3</sub> thin films were deposited by a KrF excimer PLD system with a wavelength of 248 nm (COMPex 201, Coherent, Göttingen, Germany). The dense ceramic target of Ba(Fe<sub>1/2</sub>Nb<sub>1/2</sub>)O<sub>3</sub> was placed at a rotating target holder in the vacuum chamber. Pt/TiO<sub>2</sub>/SiO<sub>2</sub>/Si substrates were used and mounted on a rotating heater during deposition. Ba(Fe<sub>1/2</sub>Nb<sub>1/2</sub>)O<sub>3</sub> thin films were deposited at temperatures varied from 823 to 923 K, with different ambient oxygen pressure in the range of 1 to 10 Pa. The energy density of the laser was fixed at about 1.5 J/cm<sup>2</sup>, and pulse repetition was 3 Hz. After deposition, the thin films were annealed at their growth temperature for 15 min in the oxygen atmosphere with the partial pressure of 3×10<sup>4</sup> Pa, and then cooled down to room temperature at the rate of 3 K/min.

The crystalline phases of Ba(Fe<sub>1/2</sub>Nb<sub>1/2</sub>)O<sub>3</sub> thin films were determined by X-ray diffraction (XRD, D/max 2550PC, RIGAKU, Tokyo, Japan) using Cu K $\alpha$  radiation ( $\lambda=1.5406$  Å) at room temperature. The surface morphologies were obtained by atomic force microscopy (AFM, Veeco diInnova, Santa Barbara, CA, USA) with tapping mode. For characterization of the electric properties, Au top electrodes of 0.3 mm in diameter were deposited through a mask by ion sputtering. The dielectric properties of the thin films were measured by a precision LCR meter (4284A, Hewlett-Packard Co., Palo Alto, CA, USA) with the temperature controller.

## 2 Results and discussion

The XRD patterns of Ba(Fe<sub>1/2</sub>Nb<sub>1/2</sub>)O<sub>3</sub> thin films deposited at 823 and 923 K with ambient oxygen pressures of 1 and 10 Pa are shown in Figure 1. A single phase perovskite structure with cubic symmetry is indicated in all thin films. Obvious peak shift to the lower angle is observed for the thin films deposited at lower ambient oxygen pressure, denoted as 2 and 4 in the Figure 1, which indicates larger lattice constants and possible crystal structure distortion in

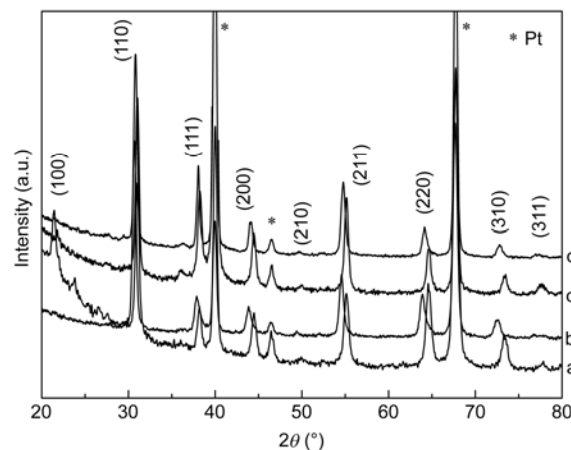


**Figure 1** XRD patterns of Ba(Fe<sub>1/2</sub>Nb<sub>1/2</sub>)O<sub>3</sub> thin films deposited at different substrate temperature of 823 and 923 K with oxygen pressure varied from 1 to 10 Pa. (a) 823 K, 10 Pa; (b) 823 K, 1 Pa; (c) 923 K, 10 Pa; (d) 923 K, 1 Pa.

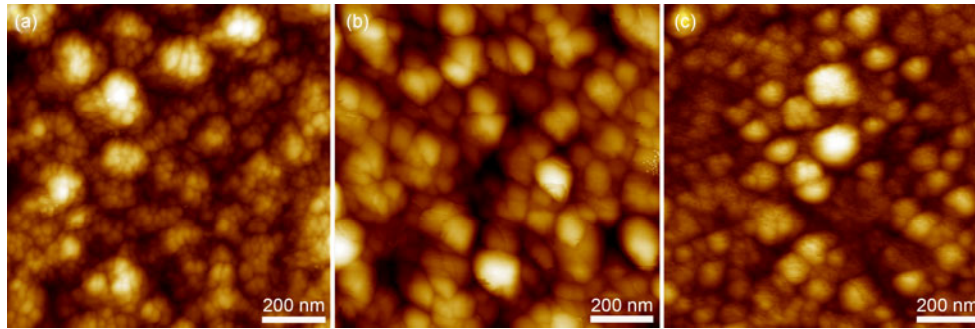
these thin films. The dependence of the crystal structure of thin films on the ambient oxygen pressure has been reported before [18]. No obvious peak shift is suggested in thin films 1 and 3, which indicated little impact on the crystal structure distortion of the substrate temperature. Meanwhile, intensified and sharper peaks are observed in the thin films 3 and 4, which indicate improved crystallization in the thin films with increasing the substrate temperature.

Figure 2 shows the surface morphologies of Ba(Fe<sub>1/2</sub>Nb<sub>1/2</sub>)O<sub>3</sub> thin films deposited at different temperature with the same ambient oxygen pressure of 10 Pa and pulse repetition of 3 Hz. The AFM images indicate that Ba(Fe<sub>1/2</sub>Nb<sub>1/2</sub>)O<sub>3</sub> thin films are well crystallized and crack-free. Obvious increase in the grain size is observed when the substrate temperature increases from 823 to 923 K. The average grain size for the thin films deposited at 823 K is about 20 nm, while the value increases to about 60–80 nm and 70–90 nm for the ones deposited at 873 and 923 K, respectively. It is noted that the root-mean-square values of surface roughness increases from 4.8 nm for the thin film deposited at 823 K to 9.8 nm for the one deposited at 923 K over the 2×2 μm scan area.

For the three-dimensional island nucleation and growth, also known as Volmer-Weber growth [19], the nucleation and growth for a given cluster is governed by its total free energy, which includes the surface/interface free energy and the change of the volume free energy on condensation of the cluster. For heterogeneous nucleation in a vapor deposition, the shape of the nucleus must be considered, which makes the change of the free energy [20],

$$\Delta G = -V_c \Delta G_v + A_{cv} \gamma_{cv} + A_{cs} \gamma_{cs} - A_{sv} \gamma_{sv}, \quad (1)$$

where c, v and s refer to the cluster, vapor and substrate, respectively;  $V_c$  is the volume of the spherical cap;  $A_{cv}$ ,  $A_{cs}$  and  $A_{sv}$  are the areas of the cluster/vapor, cluster/substrate



**Figure 2** (Color online) The influence of the substrate temperatures (a) 823, (b) 873 and (c) 923 K on the surface morphologies of Ba(Fe<sub>1/2</sub>Nb<sub>1/2</sub>)O<sub>3</sub> thin films, when the ambient oxygen pressure is 10 Pa. The scan area is 1000 nm×1000 nm.

and substrate/vapor interfaces; and  $\gamma_{cv}$ ,  $\gamma_{cs}$  and  $\gamma_{sv}$  are the corresponding interfacial free energy. The total interfacial energy is proportional to  $r^2$ , where  $r$  is the radius of spherical nucleation. While the volume free energy per unit volume of the cluster can be written as

$$\Delta G_v = -\frac{kT}{\Omega} \ln\left(\frac{P}{P_e}\right), \quad (2)$$

to a first approximation, where  $P$  is the pressure of the arriving atoms,  $P_e$  is the equilibrium vapor pressure of the film atoms,  $k$  is Boltzmann's constant,  $T$  is the absolute temperature and  $\Omega$  is the atomic volume of the film atoms. The critical cluster size is defined by setting the derivative of the free energy with respect to cluster size to zero, leading to a critical radius of

$$r^* = \frac{-2(a_1\gamma_{cv} + a_2\gamma_{cs} - a_3\gamma_{sv})}{3a_3\Delta G_v}, \quad (3)$$

where  $a_1$ ,  $a_2$  and  $a_3$  are constants depending on the shape of the nuclei. In the present thin film and substrate system, the critical cluster size mainly depends on  $\Delta G_v$  term, as just little control is conducted over the surface and interface term. So according to eqs. (2) and (3), both increased atom deposition rate and reduced substrate temperature will increase the supersaturation, leaving a decrease in the critical cluster size and in the total free energy barrier for cluster

nucleation. As indicated in Figure 2, much smaller grains are formed at low substrate temperature.

The discussion on the Volmer-Weber growth is based on the balance between growth and dissolution processes for a given cluster. However, in PLD, the energy of the ejected species in the plume is another factor that has a dominant effect on the nucleation and growth of the thin films. Increasing the energy of the deposition flux has a similar effect with increasing the substrate temperature. As shown in Figure 3, three thin films are deposited with various oxygen pressures at 823 K. With the decreased oxygen pressure, the average energy of ejected species in the plume is upgraded significantly by fewer collisions with the ambient gas, which provide extra energy for nucleation and results in much larger grains. The effect of increased oxygen pressure is similar to the decreased deposition temperature, except that the surface roughness of the thin films barely affected by variation of the ambient oxygen pressure. It is because the increased substrate temperature has additional effect of increasing the surface diffusion coefficient of the absorbed vapor atoms. When the substrate temperature is as high as 923 K, strong surface diffusion is responsible for the obvious grain coarsen observed in Figure 2(c).

Further investigation shows that the impacts of the substrate temperature and ambient oxygen pressure on the growth dynamics and surface morphologies of Ba(Fe<sub>1/2</sub>Nb<sub>1/2</sub>)O<sub>3</sub> thin films are not independent with each other. Figure 4(a)

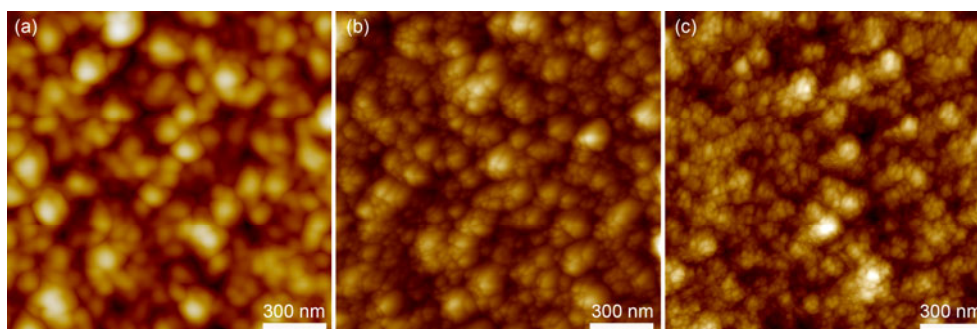


**Figure 3** (Color online) Surface morphologies of Ba(Fe<sub>1/2</sub>Nb<sub>1/2</sub>)O<sub>3</sub> thin films deposited at 823 K with various ambient oxygen pressure of (a) 1, (b) 5, and (c) 10 Pa. The scan area is 1500 nm×1500 nm.

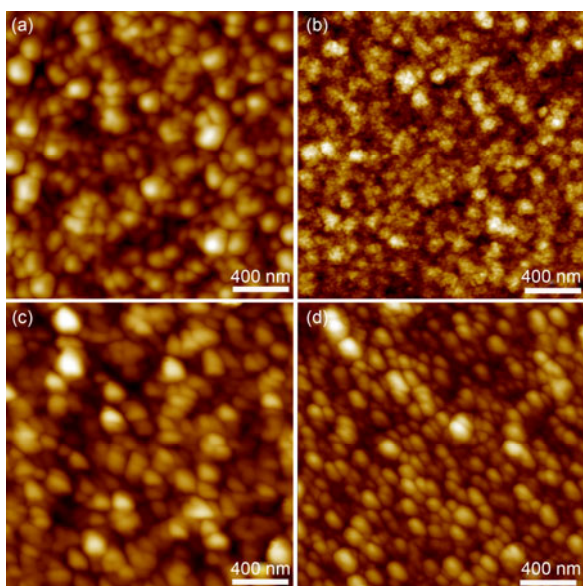


**Figure 4** (Color online) The comprehensive effects of the substrate temperature and ambient oxygen pressure on the growth of  $\text{Ba}(\text{Fe}_{1/2}\text{Nb}_{1/2})\text{O}_3$  thin films. (a), (b) Deposited at 823 K with ambient oxygen of 1 and 10 Pa, respectively; (c), (d) deposited at 923 K with ambient oxygen of 1 and 10 Pa, respectively. The scan area is  $2000\text{ nm}\times 2000\text{ nm}$ .

and (c) shows the surface morphologies of thin films deposited with ambient oxygen pressures of 1 Pa with the substrate temperature of 823 and 923 K, respectively. No obvious change in grain size is suggested, which suggests that sufficient energy has been provided by the ejected species as the ambient oxygen pressure is low. Oppositely, apparent difference in grain size is exhibited in Figure 4(b) and (d), which are deposited at 823 and 923 K with ambient oxygen pressure of 10 Pa. As we discussed before,  $r^*$  increases as the substrate temperature increases or ambient oxygen pressure decreases. Meanwhile, the possibility for forming a stable solid nucleus is decreasing as energy barrier  $\Delta G^*$  increases as well. So with high substrate temperature, the decreased ambient oxygen pressure has a weak impact on the grain size of thin films and results in a less dense surface morphology. For pulsed laser deposited  $\text{Ba}(\text{Fe}_{1/2}\text{Nb}_{1/2})\text{O}_3$  thin films, the optimized ambient oxygen pressure is 10 Pa. With low substrate temperature as 823 K, small grains could be expected, while with high temperature, dense morphology could be obtained.

Figure 5 shows the temperature dependence of the dielectric constant and loss of present thin films deposited with various ambient oxygen pressures at 823 K. As temperature below 150 K, the dielectric constant of  $\text{Ba}(\text{Fe}_{1/2}\text{Nb}_{1/2})\text{O}_3$  thin films increases with decreasing deposited oxygen pressure. The result is consistent with the crystal structure distortion in the thin films that has been reported earlier [18]. Larger structure distortion in the thin films is expected with lower deposited oxygen pressure as the existence of the oxygen deficiencies, which could be the reason for the higher dielectric constant. Meanwhile, the oxygen deficiencies

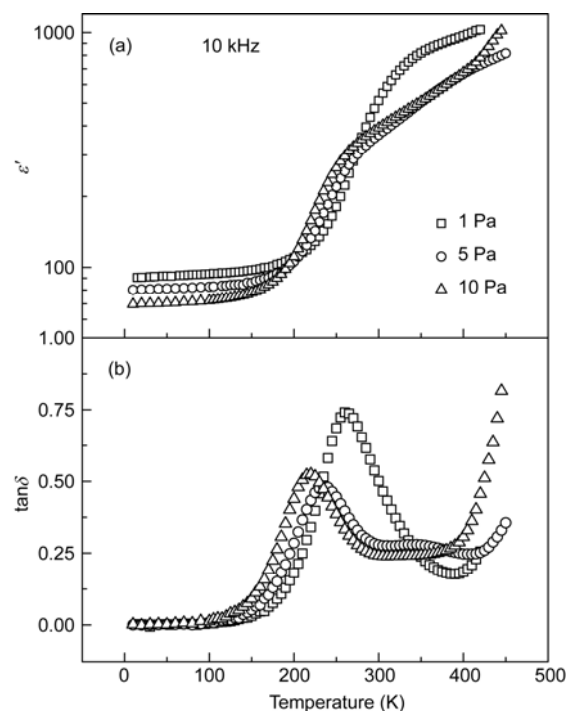


**Figure 5** The temperature dependence of the (a) dielectric constant and (b) dielectric loss of  $\text{Ba}(\text{Fe}_{1/2}\text{Nb}_{1/2})\text{O}_3$  thin films deposited with various ambient oxygen pressure under the frequency of 10 kHz.

contribute to the leakage in the thin film greatly, which becomes more obvious with increasing temperature. As shown in Figure 5(b), the dielectric loss of  $\text{Ba}(\text{Fe}_{1/2}\text{Nb}_{1/2})\text{O}_3$  thin films deposited with oxygen pressure of 1 Pa is much higher than those of the other two around the room temperature. Besides, similar dielectric constant and loss are observed for the thin films deposited with 5 and 10 Pa. The dielectric constants for  $\text{Ba}(\text{Fe}_{1/2}\text{Nb}_{1/2})\text{O}_3$  thin films deposited at 823 K are much lower than expected as the bulk ceramic exhibits giant dielectric constant, which is closely related to poor crystallization indicated by Figure 1.

Figure 6 shows the influence of deposited temperature on the dielectric properties of  $\text{Ba}(\text{Fe}_{1/2}\text{Nb}_{1/2})\text{O}_3$  thin films with the same deposited oxygen partial pressure of 10 Pa. A great increase of dielectric constant over the whole temperature range is observed when the deposited temperature increased from 823 to 923 K. Meanwhile, the dielectric loss is decreased about two thirds over the temperature range of 280 to 370 K. Much better dielectric properties of the thin film deposited at elevated temperature is attributed to improved crystallization, much larger grains and denser morphology. The dielectric constant for  $\text{Ba}(\text{Fe}_{1/2}\text{Nb}_{1/2})\text{O}_3$  thin films deposited at elevated temperatures is 2495 at 298 K (10 kHz), while the dielectric loss is around 0.084.

### 3 Conclusion

In summary, the substrate temperature and ambient oxygen

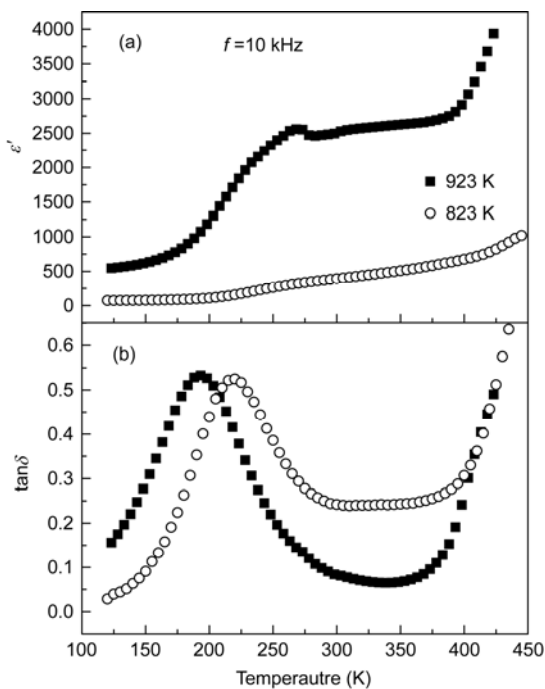


**Figure 6** The impact of the substrate temperature on the (a) dielectric constant and (b) loss of Ba(Fe<sub>1/2</sub>Nb<sub>1/2</sub>)O<sub>3</sub> thin films. The typical frequency is 10 kHz.

pressure exhibit the great impacts on the surface morphology and nucleation and growth process of Ba(Fe<sub>1/2</sub>Nb<sub>1/2</sub>)O<sub>3</sub> thin films prepared on Pt/TiO<sub>2</sub>/SiO<sub>2</sub>/Si substrates by PLD. Generally, larger grains are favored by the decreased oxygen pressure or increased substrate temperature. A dense surface morphology could be obtained when the substrate temperature is 923 K and the ambient oxygen is 10 Pa. The dielectric properties of the thin films are also shown direct dependence on the substrate temperature and ambient oxygen pressure. A great improvement is observed for the thin film deposited by the optimized condition.

*This work was supported by the National Natural Science Foundation of China (50832005 and 51202215). The acknowledgements go to Professor Chen C L at Department of Physics, University of Texas at San Antonio for his valuable discussion and suggestions.*

**Open Access** This article is distributed under the terms of the Creative Commons Attribution License which permits any use, distribution, and reproduction in any medium, provided the original author(s) and source are credited.

- Zhang M N, Xu K B, Wang G J, et al. Dielectric anomalies in CaCu<sub>3</sub>Ti<sub>4</sub>O<sub>12</sub> at high temperatures. *Chin Sci Bull*, 2013, 58: 713–716
- Homes C C, Vogt T, Shapiro S M, et al. Optical response of high-dielectric-constant perovskite-related oxide. *Science*, 2001, 293: 673–676
- Wu J B, Nan C W, Lin Y H, et al. Giant dielectric permittivity observed in Li and Ti doped NiO. *Phys Rev Lett*, 2002, 89: 217601
- Wang Z, Chen X M, Ni L, et al. Dielectric abnormalities of complex perovskite Ba(Fe<sub>1/2</sub>Nb<sub>1/2</sub>)O<sub>3</sub> ceramics over broad temperature and frequency range. *Appl Phys Lett*, 2007, 90: 022904
- Liu Y Y, Chen X M, Liu X Q, et al. Dielectric relaxation in Ca(Fe<sub>1/2</sub>Nb<sub>1/2</sub>)O<sub>3</sub> complex perovskite ceramics. *Appl Phys Lett*, 2007, 90: 262904
- Chen L, Chen C L, Lin Y, et al. High temperature electrical properties of highly epitaxial CaCu<sub>3</sub>Ti<sub>4</sub>O<sub>12</sub> thin films on (001) LaAlO<sub>3</sub>. *Appl Phys Lett*, 2003, 82: 2317–2319
- Lunkenheimer P, Bobnar V, Pronin A V, et al. Origin of apparent colossal dielectric constants. *Phys Rev B*, 2002, 66: 052105
- Liu Y, Withers R L, Wei X Y. Structurally frustrated relaxor ferroelectric behavior in CaCu<sub>3</sub>Ti<sub>4</sub>O<sub>12</sub>. *Phys Rev B*, 2005, 72: 134104
- Wang C C, Zhang L W. Polar relaxation related to localized charge carriers in CaCu<sub>3</sub>Ti<sub>4</sub>O<sub>12</sub>. *Appl Phys Lett*, 2007, 90: 142905
- Ni L, Chen X M. Dielectric relaxations and formation mechanism of giant dielectric constant step in CaCu<sub>3</sub>Ti<sub>4</sub>O<sub>12</sub>. *Appl Phys Lett*, 2007, 91: 122905
- Li M, Sinclair D C, West A R. Extrinsic origins of the apparent relaxorlike behavior in CaCu<sub>3</sub>Ti<sub>4</sub>O<sub>12</sub>. *J Appl Phys*, 2011, 109: 084106
- Zhang W, Wang Z, Chen X M. Crystal structure evolution and local symmetry of perovskite solid solution Ba[(Fe<sub>1/2</sub>Nb<sub>1/2</sub>)<sub>1-x</sub>Ti<sub>x</sub>]O<sub>3</sub>. *J Appl Phys*, 2011, 110: 064113
- Lowndes D H, Geohagan D B, Puzosky A A, et al. Synthesis of novel thin-film materials by pulsed laser deposition. *Science*, 1996, 273: 898–903
- Willmott P R, Huber J R. Pulsed laser vaporization and deposition. *Rev Mod Phys*, 2000, 72: 315–328
- Jun B E, Kim Y S, Park H J, et al. Effects of ambient oxygen pressures and substrate temperatures in pulsed laser deposition Zn<sub>0.85</sub>Li<sub>0.15</sub>O thin films. *Thin Solid Films*, 2008, 516: 5266–5271
- Orgiani P, Ciancio R, Galdi A, et al. Physical properties of La<sub>0.7</sub>Ba<sub>0.3</sub>MnO<sub>3</sub>-d complex oxide thin films grown by pulsed laser deposition technique. *Appl Phys Lett*, 2010, 96: 032501
- Zhang W, Li L, Chen X M. Effects of oxygen vacancy on ferroelectricity in Ba(Fe<sub>1/2</sub>Nb<sub>1/2</sub>)O<sub>3</sub> thin films grown by pulsed laser deposition. *J Appl Phys*, 2009, 106: 104108
- Zhang W, Li L, Chen X M. Oxygen pressure dependence of structure and electrical properties of pulsed laser deposited Ba(Fe<sub>1/2</sub>Nb<sub>1/2</sub>)O<sub>3</sub> thin films. *J Appl Phys*, 2010, 108: 044104
- Chrisey D B, Hubler G K. *Pulsed Laser Deposition of Thin Films*. New York: John Wiley & Sons, 1994
- Porter D A, Easterling K E. *Phase Transformations in Metals and Alloys*. 2nd ed. UK: Chapman & Hall, 1993